JOURNAL OF AERONAUTICS AND SPACE TECHNOLOGIES
(ISSN : 1304-0448)
January 2019 Volume 12 Number 1
www.jast.hho.edu.tr

Research Article

Frequency Analysis of Launch Vehicle Oscillation Absorbent Configuration on Performance of Liquid Propellant Engine

Seyed Alireza Jalali CHIMEH[1], Hassan Karimi Mazareh SHAHI[2]

Mohammad Shafiei DEHAJ[3]

[1] *K. N. Toosi University of Technology, Tehran, Iran alireza.jalali@mail.kntu.ac.ir*

[2] *K. N. Toosi University of Technology, Tehran, Iran, karimi@kntu.ac.ir*

[3] *Dept. of Engineering, Vali-e-asr University, Rafsanjan, Iran, m.shafiey@vru.ac.ir*

Article Info

Received: *April 3, 2018*
Accepted: *January 14, 2019*
Online: *January 23, 2019*

Keywords: Propulsion-Structure Interaction (Pogo), Pogo Stability, Accumulator, Dynamic Simulation, Liquid Propellant Engine (LPE)

Abstract

Pogo phenomenon is considered as low-frequency instability at system level in heavy satellite launchers. This instability results from the frequency interactions between structure and propulsion subsystems. To compensate for or prevent the occurrence of this instability in a satellite launcher, an element that reduces the frequency interaction effects of these two systems is used. This element, which is known as 'accumulator', absorbs the pogo vibrations in satellites. In this paper, by dynamically modeling the engine elements (tank, supply line, accumulator, pump, and thrust chamber), and by considering the connection of structure to engine at two points of tank and pump, the effects of the accumulator element and parameters on the natural frequency of the propulsion system have been investigated and the considerations related to operating conditions and the placement of this element along the supply line of the propulsion system have been determined. The findings indicate that placing the accumulator near the pump assembly and along the suction path reduces the natural frequency of the propulsion system; which contributes to a greater stability of the satellite launcher. With the increase in the compliance and inertance of accumulator, accumulator's influence on the natural frequency of the propulsion system becomes more significant.

To Cite This Article: S.A.J. Chimeh, H.K.M. Shahi, M.S. Dehaj "Frequency Analysis of Launch Vehicle Oscillation Absorbent Configuration on Performance of Liquid Propellant Engine" Journal of Aeronautics and Space Technologies, Vol. 12, No. 1, pp. 109-120, Jan. 2019.

Fırlatma Aracı Salınım Absorb Konfigürasyonunun Sıvı Yakıtlı Roket Performansına Etkisinin Frekans Analizi

Makale Bilgisi

Geliş: *4 Nisan 2018*
Kabul: *14 Ocak 2019*
Yayın: *23 Ocak 2019*

Anahtar Kelimeler: İtki-Yapı Etkileşimi (Pogo), Pogo Kararlılığı, Akümülatör, Dinamik Simülasyon, Sıvı Yakıtlı Roket (LPE)

Öz

Büyük uydu fırlatıcılarda Pogo olgusu düşük frekanslı bir dengesizlik seviyesi olarak görülür. Bu dengesizliğin sebebi yapısal ve yakma-itki sistemlerinin frekansları arasındaki değişim ve etkileşimdir. Bu kuvvet dengesizliğinin oluşumunu engellemek veya etkisini azaltmak için uydu fırlatma sisteminde bir element kullanılır. "Akümülatör" olarak da adlandırılan bu element Pogo titreşimlerini uydu yapısında absorbe eder. Bu çalışmada, akümülatörün etkisi ve itki sisteminin doğal frekans üzerindeki etkisi, motora ait dinamik modellemeler yardımıyla (tank, besleme sistemleri, akü, pompa ve itki halkası) ve motorun ana yapıya bağlandığı noktalar dikkate alınarak motorun nasıl konumlanması gerektiği ve sistemin tepkisi ölçülmüştür. Bu sayede varılan bulgular değerlendirildiğinde oluşan sonuçlar şunu göstermektedir ki, akümülatörün pompanın hemen yanına veya yakınına yerleştirilmesi, emilim yolunda kullanılan tüplerle birlikte, itki sisteminin yarattığı doğal frekansın azalmasına yardımcı olmaktadır ve bu da istenildiği üzere bütün yapının daha stabil bir hal almasında ve özellikle uydunun fırlatma anına yardımcı olmaktadır. Akümülatör ve ana yapı arasındaki uyumluluktaki bu artış ile akümülatörün itki sisteminin doğal frekansı üzerindeki etkisi de daha dikkate değer bir hal almıştır.

1. INTRODUCTION

In the early launches of heavy satellite carriers, a phenomenon emerged during flight which amazed the designers and engineers. This phenomenon, which initiated a kind of instability, was called "pogo phenomenon." This low-frequency phenomenon occurs as a result of longitudinal oscillations in the structure of satellite carriers at different times during the flight. These low-frequency oscillations may also be observed in engine's thrust and measured pressure from the propellant supply system. Pogo vibrations have also been observed in manned launches; this brings up a very important dynamic stability issue, which should be investigated and dealt with for the sake of crew safety, because longitudinal oscillations increase the level of acceleration applied to crew's cabin beyond the allowed limit. Therefore understanding this phenomenon and knowing the degree of these oscillations can be helpful in reducing and eliminating these unwanted accelerations. The American Apollo/Saturn launcher and the European Diament B launcher are some of the satellite launchers that have exhibited this type of instability. A Pogo phenomenon is also famed to self-exciting low-frequency vibrations, resulting from the closed-loop interactions between the longitudinal vibrations of satellite carrier and propulsion system [1]. This phenomenon is illustrated in Fig. 1.

In this closed-loop process, random vibrations (e.g. resulting from aerodynamics, combustion noises or changes in fluid flow rates) cause pressure fluctuations to be produced at the end of tank structures. After affecting the operating fluid, these fluctuations are transferred to the engine via propulsion supply lines; and as they pass through the propulsion system, they transform into the thrust force fluctuations, which can enhance the structural vibrations. Random vibrations may have no apparent source and remain in the system as uncertainties, such as the likelihood of the failure in injectors or unwanted leakage in the engine's hydraulic circuit or not meeting the fabrication tolerances; however, certain engine elements may themselves produce some sort of vibrations; which in this case, necessary examinations should be performed before using these elements. One of these elements is the actuator of the active control system (e.g. propellant utilization system or apparent velocity regulation system). This kind of control system, due to its nature and algorithm of operation, causes momentary or continuous changes in the flow rate of propellant (fuel or oxidizer) by sending commands to the actuator within the engine; and these flow rate variations may initiate pogo instabilities in the liquid propulsion engine

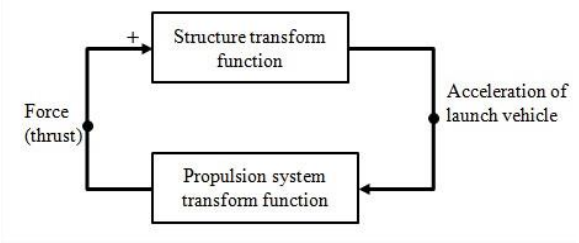

Figure 1. Closed-loop process schematic of Pogo phenomenon. [1]

A means of preventing this important phenomenon from occurring during flight is to use a tool that inhibits such frequency interactions. This element, which keeps the natural frequency of the system away from the lowest natural frequency of structure modes during flight, is called "accumulator". Accumulators are commonly used in the supply lines of propulsion systems with the longest length [2, 3]. Following the first occurrence of pogo phenomenon, Rubin used flight information analysis to investigate this phenomenon [4]. During the 1970s, designers were preoccupied with identifying this phenomenon, as the most crucial problem; and many research works, on a case basis, were conducted on Atlas [5] and Delta [6] rockets. In 1991, Qizheng et al. [7] explored the effective parameters in this phenomenon by modeling and analyzing the stability and reliability of the pogo phenomenon. The dynamic modeling and analysis of pogo phenomenon was conducted by Oppenheim et al [8] in 1994. In 2011, Zhao et al [9] studied the effects of various parameters on the pogo phenomenon. They investigated the pogo arising from engine coupling. In this research, they employed the linear model presented by Oppenheim [8] to model the pogo phenomenon for a hypothetical engine and engine's frame. To evaluate the underlying causes of pogo vibrations, extensive studies were conducted on the parameters that influence this phenomenon, including the cavitations characteristics of pumps [10, 11]. Yan Hai [12] and his team in 2009 obtained an optimal position for installing accumulator, but the analysis on parameters is not thorough and it neglects the influence of accumulator inertance. In 2012, Niu Zexiong et al [13] established a new model of suction line. But they did not focus on the influence of accumulator's parameters on frequency or coupled system's stability. In 2014, Yuan et al [14] obtained a matrix algorithm to determine the stability of POGO. To study effective methods of avoiding POGO instability, Li et al. [15] starts with a thorough research on effect of parameters on natural frequency of propulsion system in liquid rocket. They analyzed stability of coupled structure-propulsion system by using adopting the method of critical damping ratio. Also they presented an optimum position for installation of accumulator. In 2015, Shafiey et al [16] presented a mathematical model

for an open-cycle engine to predict the transient behavior of engine components, in his work, Rubin equations were used to characterize the operation of separate engine units during shutdown process. They obtained the pressure changes of the combustion chamber and determined the cutoff impulse, they saw some oscillations in cutoff impulse that may appear with accumulator effect in shutdown phase but did not study directly the accumulator effects for this phase of operation, in LPEs.

This paper starts with the establishment of dynamical model for propulsion system via the method of transfer matrix. Main goal is to investigate the sensitivity of a liquid propulsion system's frequency variations to the placement of an accumulator element along one of the propellant flow paths and the volumetric characteristics of the accumulator, and to determine these specifications for a better compensation and control of pogo phenomenon. Finally, with considering of inertance of accumulator in the proceeding equations, it is proposed the better position for this device is in propellant feed line

2. DYNAMIC MODEL OF THE LIQUID PROPULSION SYSTEM

The liquid propulsion system in satellite launchers produces the driving force for the launch vehicle. The induced vibrations in the propulsion system lead to changes in the thrust force produced by the system. Thus, the propulsion system is inevitably affected by a satellite launcher's acceleration-related oscillations, and by interacting with the launcher structure, it can lead to pogo phenomenon. Therefore it is essential to investigate the effects of likely vibrations on the liquid propulsion system. In this paper, the role of accumulator in the engine assembly, as an element used for compensating the pogo vibrations, is investigated. In launch vehicles, the pogo compensation element is generally placed along a path with a high length-to-diameter ratio and where the propagation of pressure and acceleration-related oscillations in fluid cannot be ignored due to the considerable length of the route. Therefore, for studying the frequency effects, it is sufficient to explore one line of the propulsion system's main propellant supply lines. Thus, a hydraulic circuit of the examined assembly is considered, as in Figure 2. This propulsion system path consists of five major elements: propellant tank, main supply line (divided into Sections 1 and 2), accumulator element, pump set ('s' and 'd' indicate suction at pump inlet and discharge at pump outlet, respectively), and the discharge line from pump toward the combustion chamber and thrust chamber.

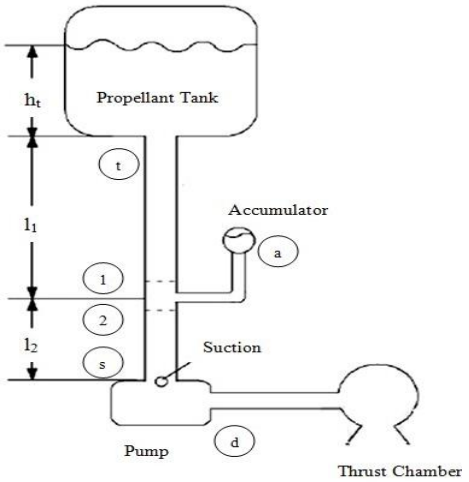

Figure 2. Hydraulic circuit of propulsion system path.

For the dynamic modeling of this assembly, the governing equations of elements should be written separately; and then by coupling the equations together, the overall set of equations for the whole system can be derived. Then by using Laplace transformation, the natural frequency of the system can be calculated. To investigate the effect of the accumulator element, the natural frequencies of the mentioned assembly are computed with the presence and absence of this element.

2.1. Propellant Tank

In order to calculate the pressure applied to the end of tank (inlet to the main line) due to the launch vehicle's acceleration [2, 3, and 4] the equation for the balance of forces at the end section of tank is written as

$$p_t = \rho h_t \ddot{x}_t \tag{1}$$

In this equation, subscript's denotes the end of tank, ρ is the density of fluid inside the tank, h_t is the height of fluid within the tank at the moment, and acceleration of the flying system is the $\ddot{x}_t$.

2.2. Supply Line (From Tank to Pump Suction)

For modeling the propellant supply lines of Path 1 and Path 2 according to Figure 2 by assuming one-dimensional, incompressible and non-viscous fluid [18], the governing conditions of fluid are expressed as follows:

$$\frac{\partial v}{\partial t} + v_0 \frac{\partial v}{\partial x} + \frac{1}{\rho}\frac{\partial p}{\partial x} = 0 \tag{2}$$

$$\frac{\partial p}{\partial t} + v_0 \frac{\partial p}{\partial x} + C_0^2 \frac{\partial v}{\partial x} = 0 \tag{3}$$

By assuming that, under fluctuating conditions and when disturbances are created during the nominal operating phase, the changes of velocity along the element's longitudinal direction can be ignored versus the changes of velocity with respect to time in Eq. 2 and also assuming that the same condition holds for pressure changes in Eq. 3, the obtained equations can be written in compact form. Thus, by using the Laplace-taking procedure and eliminating the velocity from the equations, the following equation can be obtained.

$$\begin{cases} v(x,s) = \dfrac{-1}{\rho s}\dfrac{dp}{dx} \\ s^2 p(x,s) + C_0^2 \dfrac{d^2 p}{dx^2} = 0 \end{cases} \tag{4}$$

By solving this equation and substituting $s = i\omega$, defining the wave number as $\beta = \omega / C_0$ and by applying the boundary conditions of Table 1, and considering the TLM method [19] for analogy of hydraulic systems, set of Equations (5) is obtained.

Table 1. Boundary conditions of upstream and down stream.

upstream	Down stream
$v(0) = \dot{w}_u / \rho A$	$v(1) = \dot{w}_d / \rho A$
$p(0) = p_u$	$p(1) = p_d$

$$\begin{cases} p_{do} = (\cos(\beta l))\, p_u - sL\,[\sin(\beta l)/\beta l]\,\dot{w}_u \\ \dot{w}_{do} = [(\beta l / sL)\sin(\beta l)]\, p_u + (\cos(\beta l))\,\dot{w}_u \end{cases} \tag{5}$$

In these equations, $L = l/Ag$ Also, 'u' and 'do' indicate the 'upstream' and 'downstream', respectively. Hence, in this method, for the modeling of the two paths 1 and 2, the equations can be written as follows

Path 1 (from tank's end to Point 1)

$$\begin{cases} p_1 = (\cos(\beta l_1))\, p_t - sL_1\,[\sin(\beta l_1)/\beta l_1]\,\dot{w}_t \\ \dot{w}_1 = [(\beta l_1 / sL_1)\sin(\beta l_1)]\, p_t + (\cos(\beta l_1))\,\dot{w}_t \end{cases} \tag{6}$$

And Path 2 (From Point 2 to pump inlet),

$$\begin{cases} p_s = (\cos(\beta l_2))\, p_2 - sL_2\,[\sin(\beta l_2)/\beta l_2]\,\dot{w}_2 \\ \dot{w}_s = [(\beta l_2 / sL_2)\sin(\beta l_2)]\, p_2 + (\cos(\beta l_2))\,\dot{w}_2 \end{cases} \tag{7}$$

2.3. Connecting and Branching Junctions

In the modeling of fluid flow in branching point, according to figure 2 a mass flow rate conservation equation is written for the inlet and outlet of the accumulator element, and equal pressures are assumed at the inlet and outlets of this point [17]. Thus, the governing equation for the splitting point between the accumulator element and the main propellant supply line, from tank to pump, are as follows:

$$\begin{cases} \dot{w}_1 = \dot{w}_2 + \dot{w}_a \\ p_1 = p_2 = p_a \end{cases} \tag{8}$$

In this equation, subscript '*a*' is used to denote the accumulator element.

2.4. Thrust Chamber

The thrust chamber is an element in which combustion occurs and the hot high-energy gases resulting from combustion are exhausted to the outside through the nozzle; and thus the potential energy of gases is converted to kinetic energy. In this element, the thrust depends on the combustion chamber pressure [17]. By considering the combustion delay time, the combustion chamber pressure is expressed as

$$p_c(t+\tau) = \frac{C^* \dot{w}_{total}}{A_{th} g} \tag{9}$$

By using Taylor expansion, a linearized pressure equation is obtained; which in the Laplace transformation process, is written as

$$(1+\tau s)\, p_c = \frac{C^* \dot{w}_{total}}{A_{th} g} \tag{10}$$

On the other hand, produced thrust from Thrust chamber can be written in following form.

$$T = A_t C_f p_c \tag{11}$$

2.5. Discharge Line from Pump Outlet to Combustion Chamber

This line in liquid propellant engine base on figure 2 is shorter than other line and the propagation of oscillations wave is very limited along the tube length, the effect of oscillations on these paths are assumed to be negligible; Therefore only the pressure loss of the line and the Fluid inertia are taken into consideration[4]. This pressure difference is written as

$$p_d - p_c = (sI_d + R_d)\,\dot{w}_d \tag{12}$$

Where I_d denotes the inertance of the discharge line and R_d is the local resistance of the discharge line [18].

2.6. Pump Set

Pump system in liquid propulsion engines used to produce the required head for the combustion chamber. The turbo-pump assembly is one of the points where the engine system connects and couples with the structure of launch vehicle. In this paper, it is assumed that the pump element frames and its connection to the structure is the reference point between engine assembly and structure. Considering the relationship between pressure difference (head), angular velocity, and pump's suction pressure [4, 16], the following equation can be written:

$$p_d - p_s = \frac{\partial H}{\partial p_s}\Delta p_s + \frac{\partial H}{\partial \dot{w}_d}\Delta \dot{w}_d + \frac{\partial H}{\partial N}\Delta N \qquad (13)$$

In view of the characteristic pump diagrams, the effects of the first two terms of Equation (13) (i.e., pressure head vs. suction pressure and pressure head vs. outlet flow rate) are greater than that of the third term. Thus, two parameters of pump gain factor and hydraulic resistance of pump are defined [4]. For a constant suction pressure, we can write

$$p_d = (m+1)\,p_s + R_p \dot{w}_d \qquad (14)$$

Where in equation (13) m and R_p is defined below

$$m = \frac{\partial H}{\partial p_s} \qquad R_p = \frac{\partial H}{\partial \dot{w}_d}$$

The rate of fluid flow through the pump system is indicated by $\dot{w}_d$. Figure 3 shows the pump's inlet and outlets. Also, considering the acceleration effects of fluid due to the motion of satellite launcher and the compliance effects of pump, the mass flow rate of fluid passing through the turbo-pump system is expressed as follows:

$$\dot{w}_d = \dot{w}_s + \rho A_s \dot{x}_s - s\rho C_b p_s \qquad (15)$$

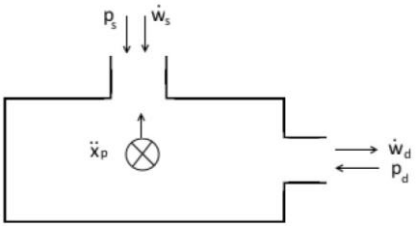

Figure 3. Pump's inlet and outlets.

2.7. Accumulator

This element is employed for the prevention of pogo phenomenon in liquid propulsion engines. The basic reason for using such a system is to absorb or reduce pressure fluctuations caused by the satellite carrier's acceleration oscillations. There are different types of accumulators, which acts via different methods. Fig. 4.a shows that schematic of this element and Fig 4.b shows schematics of accumulators that successfully suppressed pogo on various vehicles

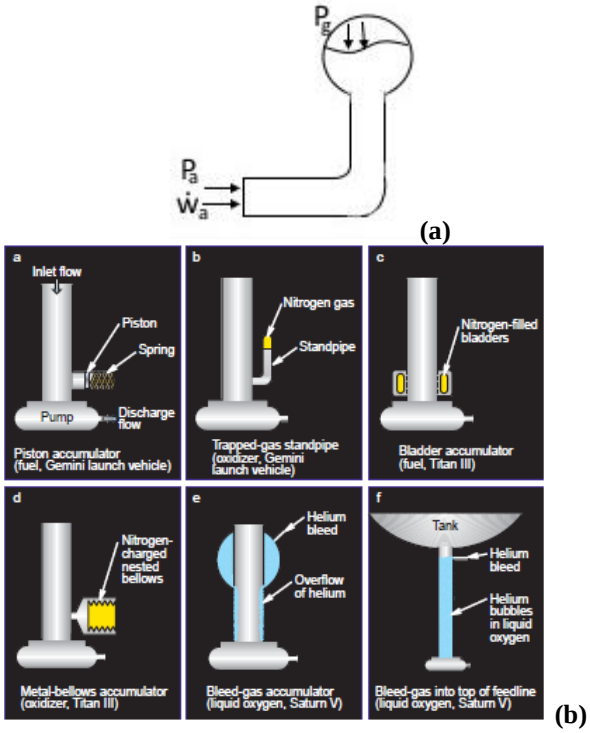

Figure 4.(a) Accumulator **(b)** Schematics of accumulators that successfully suppressed pogo on various vehicles. [8]

The governing equation for the pressure head of this element is obtained by using the equations presented in Section "*Discharge line from pump outlet to combustion chamber*"

$$p_a - p_g = (sI_a + R_a)\dot{w}_a \qquad (16)$$

The equation for the flow rate of fluid entering this element from the branch side is obtained as follows, by using the compliance concept.

$$\dot{w}_a = -sC_b p_g \qquad (17)$$

3. COUPLING OF EQUATIONS

The governing equations of the hydraulic elements shown in Fig. 2 have been presented separately and in different sections. The system of governing equations includes a combination of Equations 1, 7(a), 7(b), 8, 10, 11, 12, 13, 14, 15 and 16. In this system of equations, by omitting the pressure variables of elements from the equations, the equations can be written in state space form, as follows:

$$\begin{cases} \left[sI - A\right]\left\{\dot{w}\right\} = \left\{B\right\}\ddot{x}_p \\ T = \left\{C\right\}\left\{\dot{w}\right\} \end{cases} \tag{18}$$

In Equation (18), matrixes $\left[sI - A\right]$, $\left\{\dot{w}\right\}$, $\left\{B\right\}$ and $\left\{C\right\}$ result from the coupling of equations associated with the circuit. These matrices are defined as

$$\left[sI - A\right] = \begin{bmatrix} A_{22} & -1 & 0 \\ s\rho C_b A_{12} & -1 & 1 \\ (m+1)A_{12} & 0 & (sI_d + R) \end{bmatrix} \tag{19}$$

In this matrix, the coefficients of *A* are as follows:

$$\begin{aligned} A_{11} &= \cos(\beta l) + \kappa s L_2 \frac{\sin(\beta l_2)}{\beta l_2}\cos(\beta l_1) Z^{-1} \\ A_{12} &= -sL\frac{\sin(\beta l)}{\beta l} - \kappa s^2 L_1 L_2 \frac{\sin(\beta l_1)}{\beta l_1}\frac{\sin(\beta l_2)}{\beta l_2} Z^{-1} \\ A_{21} &= -\frac{\beta l}{sL}\sin(\beta l) + \kappa \cos(\beta l_1)\cos(\beta l_2) Z^{-1} \\ A_{22} &= \cos(\beta l) + \kappa s L_1 \frac{\sin(\beta l_1)}{\beta l_1}\cos(\beta l_2) Z^{-1} \end{aligned} \tag{20}$$

In this equation, l = l_1 + l_2 and L = L_1 + L_2, and the expressions of *Z* and *R* have been defined as follows. Also, κ has been defined as the presence or absence factor of accumulator in order to facilitate the analysis of this element's effect on the system.

$$Z = sI_a + R_a + s^{-1}C_a^{-1} \tag{21}$$

$$R = C^* / (A_t g) + R_d + R_p \tag{22}$$

The state variables considered in the equations include the mass flow rates of fluid at the inlets of supply line (tank outlet), pump and combustion chamber; which are expressed as follows:

$$\left\{\dot{w}\right\} = \left\{\dot{w}_t \quad \dot{w}_s \quad \dot{w}_d\right\}^T \tag{23}$$

Also, the coefficients matrix of B and C is expressed as

$$B = \frac{\rho h_t}{g}\frac{\varphi_t}{\varphi_p}\begin{Bmatrix} -A_{21} \\ -sC_b A_{11} + \frac{A_s}{s}\frac{g}{h_t}\frac{\varphi_p}{\varphi_t} \\ -(m+1)A_{11} \end{Bmatrix} \tag{24}$$

$$\left\{C\right\} = \left\{0 \;\; 0 \;\; A_f C_f \;\; \frac{1}{(\tau_c s + 1)}\frac{C^*}{A_t g}\right\} \tag{25}$$

4. EXTRACTING THE NATURAL FREQUENCY OF THE PROPULSION SYSTEM

In the preceding sections, the equations related to the liquid propulsion system and its elements and the coupled equations of the hydraulic circuit in Fig. 2 were presented. In this section, the set of equations associated with the propulsion system is solved in order to determine the natural frequency of the system. For this purpose, Eigen values of the system are extracted by setting to zero the determinant of the matrix of state variable coefficients.

$$\left|sI - A\right| = 0 \tag{26}$$

The solution of Equation (26) indicates that the determinant of this multi-element matrix is of the 5th order for the Laplace operator. For simplification, the inertance of the propellant supply line to the thrust chamber, which has been introduced as the discharge line, is disregarded against the inertance of other system paths, and the considered determinant is written as follows:

$$\left.\begin{pmatrix} s^4[\kappa L_1 L_2 C_a C_b l \sin(\beta l_1)\sin(\beta l_2) \\ +LI_a C_a C_b \sin(\beta l)\beta l_1 l_2] \\ +s^2[\kappa\beta l l_2 L_1 C_a \sin(\beta l_1)\cos(\beta l_2) \\ +\beta^2 l l_2 C_a I_a \cos(\beta l) l_1 \\ +LC_b \sin(\beta l)\beta l_1 l_2] \\ +\beta^2 l l_2 l_1 \cos(\beta l) \end{pmatrix}\right/ den = 0 \tag{27}$$

In this equation, 'den' is defined as

$$den = \beta^2 l\left(I_a C_a s^2 + 1\right) l_2 l_1$$

Thus, by solving Equation (27) for parameter "s" and substituting $s = i\omega$, the natural frequencies of the

propulsion system can be determined. For computing the natural frequency of the system, the vibration frequency is assumed to be very small, and it is considered that $\beta \to 0$. In this case, the natural frequency of the system, with or without the accumulator element, can be extracted.

4.1. Absence of Accumulator

In this case, expression κ in Equation (27) is set to zero and the obtained equation is solved. The solution, considered to be the natural frequency of the liquid propulsion system without the accumulator (ω^*), is represented by equation below:

$$\omega^* = \frac{1}{\sqrt{LC_b}} \tag{28}$$

As the equation indicates, the system's natural frequency totally complies with the operating conditions of the turbo-pump system and the geometrical conditions of flow paths.

4.2. Presence of Accumulator

The natural frequency of the liquid propulsion system with the accumulator element is obtained by solving Equation (27), as follows

$$\tilde{\omega}^* = \sqrt{\frac{\left[\left(L_1C_a + LC_b + I_aC_a\right) \pm \sqrt{\left(L_1C_a + LC_b + I_aC_a\right)^2 - 4\left(L_1L_2C_aC_b + LI_aC_aC_b\right)}\right]}{2\left(L_1L_2C_aC_b + LI_aC_aC_b\right)}} \tag{29}$$

As is indicated by the equation, this natural frequency is totally sensitive to the location of accumulator element, operating conditions, compliance of pump and accumulator and the inertance of accumulator.

5. RESULTS AND DISCUSSION

5.1. Sensitivity Analysis of The Effect of Accumulator on the Propulsion System's Natural Frequency

For evaluating and analyzing the effect of accumulator element on the liquid propulsion system, a non-dimensional frequency ratio Ω, which obtained by dividing equation (28) to equation (29), is introduced. To simplify the equation pertaining to the frequency ratio Ω, dimensionless parameters that appear in this equation are introduced.

$$\Omega = \frac{\tilde{\omega}^*}{\omega^*}, \qquad \eta = \frac{L_1}{L}, \qquad \lambda = \frac{I_a}{L},$$

$$1-\eta = \frac{L_2}{L}, \qquad \gamma = \frac{C_a}{C_b}$$

By using the definitions and parameters introduced above, the equation related to frequency ratio Ω is written as follows:

$$\Omega = \sqrt{\left\{\frac{\left[\left(\lambda\gamma + \eta\gamma + 1\right) \pm \sqrt{\left(\lambda\gamma + \eta\gamma + 1\right)^2 - 4\left(\lambda\gamma + \eta\left(1-\eta\right)\gamma\right)}\right]}{2\left(\lambda\gamma + \eta\left(1-\eta\right)\gamma\right)}\right\}} \tag{30}$$

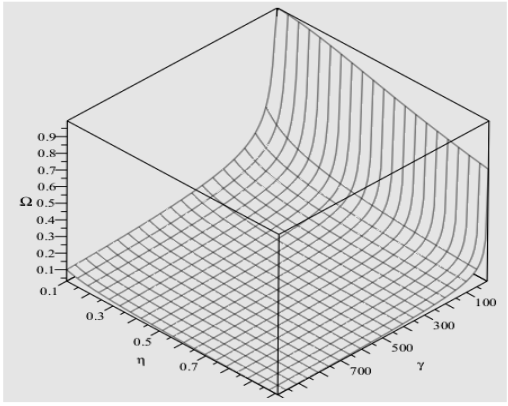

Figure 5. Influence of system's frequency ratio from variation of accumulator parameters.

Parameter λ in equation (30), which takes on a value of zero or one, has been introduced for investigating the effect of accumulator inertance. The parameters that influence the system's frequency ratio are evaluated by plotting equation (30) for the defined ranges of accumulator parameters γ (compliance ratio) and η (accumulator location). The resulting diagram (Figure 5) indicates that for small γ coefficients, and when η gives low values, the frequency ratio approaches one; which means the ineffectiveness of the accumulator. However, with the increase of accumulator's compliance ratio, the influence of accumulator location on the system's natural frequency diminishes; and this occurs for γ >150.

The sensitivity of the natural frequency ratio to its parameters is evaluated by using the derivative of equation 29 with respect to each parameter and

analyzing the effect of each parameter on the derivative value. Hence, large variations of the derivative mean the influence of these parameters on the equation, and small variations indicate the low sensitivity of the system to this parameter. In view of figure 6, for further evaluation of parameters γ and η, the sensitivity analysis of system's natural frequency can be performed for γ values less than 150.

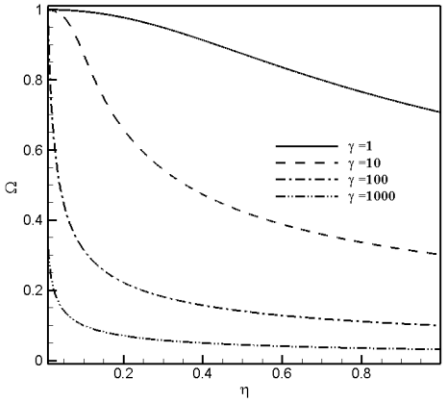

Figure 6. Projection of the system's frequency ratio onto the $\eta - \Omega$ plane.

5.2. Sensitivity of the Propulsion System's Natural Frequency to the Compliance Ratio of Accumulator

The accumulator compliance ratio, which is the ratio of accumulator's cavitations coefficient to pump's cavitation coefficient, is indicative of system performance. To investigate the sensitivity of system to this parameter, the derivative of equation (29), is taken with respect to γ and plotted for the range of 10-1000 (which has been obtained for this parameter from statistical analysis), for different accumulator-to-pump distances. The obtained graphs for two cases (with and without the consideration of accumulator inertance) have been illustrated in figure 7 and Figure 8 respectively. Figure 7 shows that sensitivity of propulsion system frequency diminishes with the increase in the γ ratio, when the accumulator location gets closer to pump. Also, figure 8 shows sensitivity of frequency ratio variations to compliance ratio for different accumulator-to-pump distances.

Similarly, when accumulator is considered to be far away from pump, the effect of compliance ratio on system frequency will be negligible and can be ignored; in general, the natural frequency of the propulsion system is fully sensitive to the changes of compliance ratio, but this sensitivity diminishes with the increase of compliance ratio. In view of figure 8, it can be realized that with the increase of compliance ratio, and when accumulator inertance is taken into consideration, the natural frequency of the propulsion system varies greatly when accumulator is far away from pump; and as the accumulator gets closer to pump, this sensitivity diminishes. In other words, when accumulator inertance cannot be ignored, the accumulator should be installed near the turbo-pump assembly in order to prevent the changes of fluid flow rate and compliance ratio from affecting the natural frequency of the propulsion system.

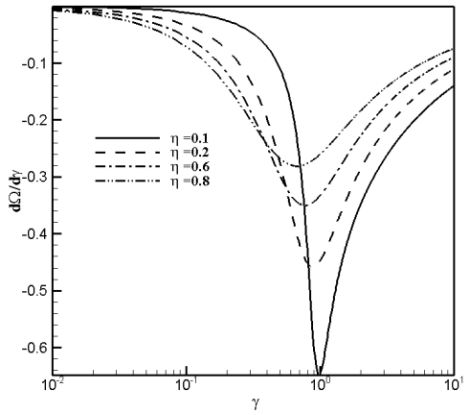

Figure 7. Sensitivity changes of frequency ratio to compliance ratio for different accumulator-to-pump distances ($\lambda = 0$).

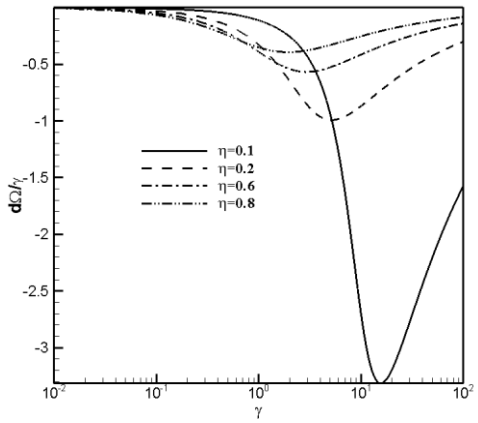

Figure 8. Sensitivity changes of frequency ratio to compliance ratio for different accumulator-to-pump distances ($\lambda = 1$).

5.3. Sensitivity of the Propulsion System's Natural Frequency to Accumulator Location

The location of accumulator, as revealed by Figs. 5 and 6, is one of the parameters that influence the natural frequency of a liquid propulsion system. Therefore, in order to explore the sensitivity of the system's natural frequency, the system sensitivity variations were analyzed by taking the derivative of Eq. 28 with respect to parameter η. The obtained diagrams have been presented in Figs. 9 and 10, for two cases (considering

or disregarding the inertance of accumulator) and for different compliance ratios.

As is indicated in Figure 9, in conditions in which the inertance of system can be ignored, the sensitivity of system's natural frequency to the increase of compliance ratio is high; and when this ratio is less than 100, the maximum sensitivity occurs at a accumulator location (η) of about 0.1. In view of Figure 10, we can say that if the inertance of accumulator is not considered, the sensitivity of natural frequency to accumulator location will diminish with the increase of compliance ratio.

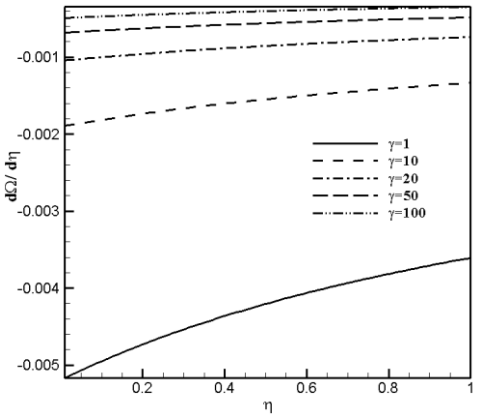

Figure 9. Sensitivity of system frequency to the location of accumulator, for different compliance ratios ($\lambda = 0$).

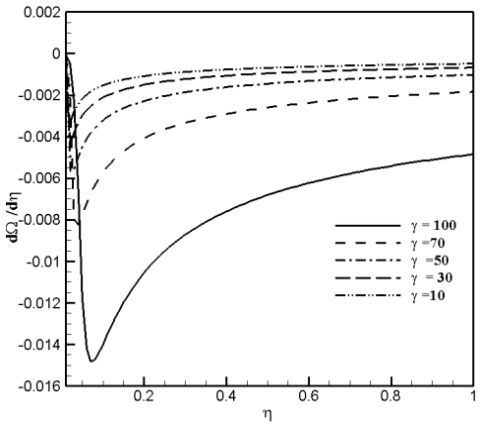

Figure 10. Sensitivity of system frequency to the location of accumulator, for different compliance ratios ($\lambda = 1$).

5.4. Validating the System's Natural Frequency Equations

To evaluate the results related to the modeling of phenomena that occur during the flight of satellite carriers, we generally need to know the conditions of the launch vehicle and the elements associated with it. Likewise, in analyzing and evaluating the pogo phenomenon, the propulsion system and the structural components of a satellite launcher are considered as two key subsystems, whose complete information must be available. The pogo phenomenon has been the focus of attention ever since it was discovered in 1960s, when the world's credible space agencies such as NASA and ESA began manufacturing a variety of satellite. Some of the papers published on this phenomenon have been presented in [2, 4, and 5]. In the present paper, we have used a set of equations whose validity for different launch vehicle has been investigated [confirmed] by [4 and 5]. To explore the effects of parameters and states mentioned in Sections 5-1 and 5-2 for a test sample, the operating conditions of a satellite carrier, whose flight information has been given in [7], are investigated here. Based on the presented information, this satellite carrier has experienced the pogo phenomenon during flight, and apparently, by using a specific accumulator system and varying the natural frequency of the propulsion system, the interference between the frequency oscillations of the two subsystems during flight has been prevented. This problem is investigated here by using Eqs. 26 and 27 and the accumulator's specifications presented in [7]. The results of this study have been illustrated in Figure 11 and table 2.

In Fig. 11, lines 1, 2, 3 and 4 respectively show the launch vehicle's natural frequency fluctuations during flight, propulsion system's natural frequency fluctuations with time in the absence of accumulator, propulsion system's natural frequency fluctuations versus flight time, with the accumulator positioned at L = L1/2, and the propulsion system's natural frequency fluctuations versus flight time, with the accumulator positioned at L = 0.9L1. This point must be told, data of lines 1 and 2 are derived from [7] and lines 3 and 4 are from our modeling and analysis.

As is observed in this figure, in the absence of an accumulator for the propulsion system, and after the elapse of 60% of flight time, the natural frequency graphs of the propulsion and vehicle interfere with each other; which may signal the occurrence of pogo phenomenon. However, when the frequency computations of the propulsion system are performed by considering an accumulator whose geometrical and spatial specifications have been given in [7], and when the accumulator element is situated near the turbo pump assembly (line 4), it is observed that the interference of natural frequency graphs of the propulsion and launch vehicle structure during flight time is eliminated and stable conditions are provided for the whole system. Furthermore, in order to evaluate the results of sensitivity analyses presented in Sections 5-1 and 5-2, the mentioned computations were also carried out for conditions L1 = 0.5L (line 3), in which the accumulator

is installed farther away from the turbo pump assembly. As Fig. 11 shows, by implementing this change of configuration, again the natural frequency graphs of the propulsion and launch vehicle structure interfere with each other during flight time. Therefore, it can be concluded that, for an accumulator, the location at which it is installed is a very important parameter, and that by improper positioning, the accumulator may lose its useful functioning.

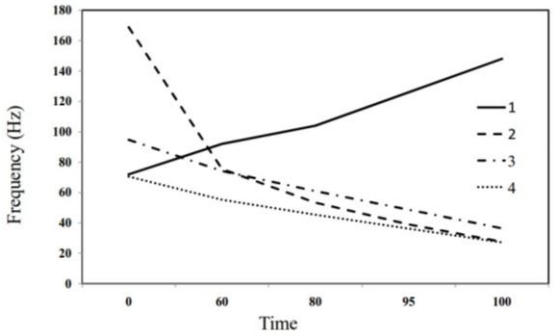

Figure 11. Comparing the natural frequency of the propulsion system with the natural frequency of the launch vehicle structure at different times and for different positions of accumulator.

Table 2. Comparison between 4 condition, 1) launch vehicle natural frequency variation during flight time, 2) propulsion system's natural frequency fluctuations with time in the absence of accumulator, 3) propulsion system's natural frequency fluctuations versus flight time, with the accumulator positioned at $L = L_1/2$ and 4) the propulsion system's natural frequency fluctuations versus flight time, with the accumulator positioned at $L = 0.9L_1$.

percentage of nominal flight duration	20%	60%	80%	95%	100%
1, Ref.[7]	82	92	104	126	148
2, Ref. [7]	123	48	36	29	28
3, present $L=0.5L_1$	83	56	46	36.9	36
4 present L=0.9L1	64	41	35.5	29.4	29

Considering the fact that the compliance factor of the turbo pumps which presented in [7] increases with time, it is clear that, coefficient γ increases as well for this sample. Therefore, with the displacement of accumulator's position, and in order to achieve the parameter γ to the value of one, according to the graph of Fig. 6, the ratio of the natural frequency of the propulsion system with accumulator to the propulsion system without accumulator should decrease. This behavior is in accordance with the specifications of engine which presented in [7] provided.

6. CONCLUSION

In this paper, the effects of different accumulator parameters on the natural frequency of a liquid propulsion system were investigated, and by applying some initial assumptions for linearizing of pump's behavior, cavitation phenomenon which effect on size of accumulator and assume very simple penumahydraulic circuit for liquid propellant engine and deriving the governing equations for different elements of the considered circuit, the equation for the liquid propulsion system's natural frequency was obtained. The sensitivities of various accumulator parameters were analyzed and presented in Figs. 7 through 10. For the purpose of validating the derived equations and the sensitivity analyses performed in Sections 5-1 and 5-2, the flight data and the information related to the elements of a specific satellite launcher were used to investigate the validity of these equations; and the analyzing the results obtained are consistent with the actual conditions.

In Fig.11 we compare some conditions of installation of accumulator with valid data and checked out of these variations on natural frequency of propulsion system. The conclusion regarding the use of an accumulator element in liquid propulsion engines and its effect on the system's natural frequency is that the installation of accumulator near the pump prevents the emergence of pogo phenomenon by keeping the natural frequency of the propulsion system away from the natural frequency of the launch vehicle structure and leads to improved stability of the whole system.

This is already explained, but the parameter calculations presented in this paper show that for liquid propulsion engines, regardless of the amount of its thrust, designers could use this calculations for engine primary layout of elements for keep the natural frequency of propulsion system on desired level, and on the other hand given that this is a systemic issue which forced to propulsion design team as a requirement so the system man could use this calculations for setting suitable constraints.

Moreover, it was found that by increasing the accumulator's compliance factor or inertance, the propulsion system's natural frequency diminishes; and when the compliance factor increases sufficiently, the influence of the installation location of accumulator system can be disregarded. This shows the great importance of the compliance coefficient; and when the inertance of an accumulator cannot be ignored without considering its installation location; the capacity ratio

should be taken as close to 1.0 as possible in order to minimize the fluctuations of natural frequency.

Nomenclature

A = Cross-sectional area, m^2
$[A]$ = Matrix of state equation
$[B]$ = Matrix of state equation
C^* = Characteristic combustion product velocity, m/s
C_a = Accumulator compliance coefficient, m^2
C_b = Pump inlet compliance coefficient, m^2
g = Gravitational constant, 9.81 m/s^2
h = Fluid height, m
I = Elements inertia, s^2/m^2
$m+1$ = Pump gain, dimensionless
R = Linear resistance for fluid dynamics, s/m^2
s = Laplace operator
w = Mass flow rate, N/s
x = Direction coordinate (movement), m
z = Impedance, s/m^2
β = Wave number, dimensionless
γ = Accumulator compliance ratio to the pump inlet
η = Accumulator wrapping length ratio to the power supply line, 1/s
κ = Coefficient accumulator element
ρ = Density, kg/m^3
τ = Time period, s
ω = Vibration frequency, Hz
ω^* = Natural frequency of the engine system without accumulator, kg/m.s
$\tilde{\omega}^*$ = Natural frequency of the engine system with accumulator, s
Ω = System natural frequency ratio

Subscripts

a = Engine element
d = Discharge
do = Fluid flow downstream
g = Accumulator gas sector
p = Pump
s = Suction
t = Propellant tank
u = Fluid flow upstream

7. REFERENCES

[1] Rasumoff, A., & Winje, R. A., "The Pogo Phenomenon: Its Causes and Cure" *In Astronautical Research*. Springer, Dordrech, pp. 307-322, 1971.

[2] Rubin, S, "Prevention of Coupled Structure-propulsion Instability (POGO)". *Journal of National Aeronautics and Space Administration* 1970.

[3] Rubin, S., "Analysis of Pogo Stability". *In Astronautical Research*, Springer, Dordrecht, pp. 113-125, 1973.

[4] McKenna, K., Walker, J., Winje, R., "A model for studying the coupled engine- airframe longitudinal instability of liquid rocket systems" *Aerospace Sciences Meetings: American Institute of Aeronautics and Astronautics* 1964.

[5] Rose, R. G., Harris, R., "Dynamic analysis of a coupled structural/pneumatic system - longitudinal oscillation for atlas vehicles". *1st Annual Meeting, Annual Meeting: American Institute of Aeronautics and Astronautics* 1964.

[6] Payne, G. J., Rubin, S., "*Suppression on the Delta Vehicle*", *Journal of National Aeronautics and Space Administration* 1974.

[7] Qizheng, W., Wanyong, G., Yongchun, G.,"POGO Stability, reliability and parameters analysis", *Astronautics Journal*, NR 2, pp. 29-47, 1991.

[8] Oppenheim, B. W., Rubin, S., "Advanced Pogo stability analysis for liquid rockets", *Journal of Spacecraft and Rockets*, Vol. 30, No. 3, pp. 360-373, 1993.

[9] Zhang, J., Wang, Q.," Parameter Study on Pogo Stability of Liquid Rockets", *Journal of Spacecraft and Rockets*, Vol. 48, No. 3, pp. 537-541, 2011.

[10] Kirk, D., Rubin, S., Brian, S.," Effects of Unsteady Pump Cavitation on Propulsion-Structure Interaction (Pogo) in Liquid Rockets", *45th AIAA/ASME/ ASCE/AHS/AS Structural Dynamics Conferences: American Institute of Aeronautics and Astronautics*, 2004.

[11] Dotson, K. W., Rubin, S., Sako, B. S., "Mission-Specific Pogo Stability Analysis with Correlated Pump Parameters", *Journal of Propulsion and Power*, Vol. 21, No. 4, pp. 619-626, 2005.

[12] Yan Hai, Fang Bo, Huang Wenhu "Research and Parameter Analysis of POGO Vibration in Liquid Rocket "*Journal of Missiles and Space Vehicles*, Vol. 6, pp. 35-40. 2009.

[13] Niu Zexiong, Dong Chaoyang, Huang Xiyuan "A new method of modeling for POGO analysis" *Journal of Structure & Environment Engineering*, Vol. 39, No. 5, pp. 29-33, 2012.

[14] Xu De-yuan, Hao Yu, Yang Qiong-liang. "Fast Matrix Algorithm for POGO Instability Prediction in Liquid rocket" *Journal of Astronautics*. 2014. Vol. 35, No. 1, pp. 21-27, 2014.

[15] Li, Hou Wang, Cong Wang, and Xiao Shi Zhang. "Analysis on Stability of POGO and Parameters of Propulsion System in Liquid Rocket." *Journal of Applied Mechanics and Materials*. Vol. 664, pp. 158-162, 2014.

[16] 2014. Shafiey, D. M., Ebrahimi, R., Karimi, H., *"*Mathematical modeling and analysis of cutoff impulse in a liquid propellant rocket engine*". Proceedings of the Institution of Mechanical Engineers, Part G: J of Aerospace Engineering*, 2015, Vol. 229, No. 13, pp. 2358-2374, 2015.

[17] Tabrizi, M. N., Chime, S. A. J., Karimi, H., "Modeling and Simulation of Open Cycle Liquid Propellant Engines", *Journal of Science and Engineering*, 2013, Vol. 1, No. 1, pp. 17-34, 2013.

[18] Fox, R.W., and Mcdonald's "Introduction to Fluid Mechanics", 9th Edition Wiley E-Text Reg Card: John Wiley & Sons, Incorporated, 2015.

[19] De Cogan, D., O'Connor W. J., Pulko, S., "Transmission Line Matrix (TLM)" *in Computational Mechanics*, CRC Press, 2005.